

NRC Publications Archive Archives des publications du CNRC

Influence of feedstock powder characteristics on the response to heat treatment of cold sprayed copper coatings

Poirier, Dominique; Kotsakis, Ioannis; Giallonardo, Jason; Yue, Steve

This publication could be one of several versions: author's original, accepted manuscript or the publisher's version. / La version de cette publication peut être l'une des suivantes : la version prépublication de l'auteur, la version acceptée du manuscrit ou la version de l'éditeur.

For the publisher's version, please access the DOI link below. / Pour consulter la version de l'éditeur, utilisez le lien DOI ci-dessous.

Publisher's version / Version de l'éditeur:

<https://doi.org/10.1007/s11666-024-01865-6>

Journal of Thermal Spray Technology, pp. 1-30, 2024-11-12

NRC Publications Archive Record / Notice des Archives des publications du CNRC :

<https://nrc-publications.canada.ca/eng/view/object/?id=f6bcb9b9-a7ec-4b70-88b3-17b308819ced>

<https://publications-cnrc.canada.ca/fra/voir/objet/?id=f6bcb9b9-a7ec-4b70-88b3-17b308819ced>

Access and use of this website and the material on it are subject to the Terms and Conditions set forth at

<https://nrc-publications.canada.ca/eng/copyright>

READ THESE TERMS AND CONDITIONS CAREFULLY BEFORE USING THIS WEBSITE.

L'accès à ce site Web et l'utilisation de son contenu sont assujettis aux conditions présentées dans le site

<https://publications-cnrc.canada.ca/fra/droits>

LISEZ CES CONDITIONS ATTENTIVEMENT AVANT D'UTILISER CE SITE WEB.

Questions? Contact the NRC Publications Archive team at

PublicationsArchive-ArchivesPublications@nrc-cnrc.gc.ca. If you wish to email the authors directly, please see the first page of the publication for their contact information.

Vous avez des questions? Nous pouvons vous aider. Pour communiquer directement avec un auteur, consultez la première page de la revue dans laquelle son article a été publié afin de trouver ses coordonnées. Si vous n'arrivez pas à les repérer, communiquez avec nous à PublicationsArchive-ArchivesPublications@nrc-cnrc.gc.ca.

Influence of feedstock powder characteristics on the response to heat treatment of cold sprayed copper coatings

Ioannis Kotsakis^{*a}, Dominique Poirier^b, Jason D. Giallonardo^c, Stephen Yue^a

a: Department of Mining and Materials Engineering, McGill University, 3610 University Street, Montreal, H3A 0C5, Quebec, Canada

b: National Research Council of Canada, 75 De Mortagne Blvd, Boucherville, J4B6Y4, Quebec, Canada

c: Nuclear Waste Management Organization of Canada, 22 St. Clair Avenue East, 4th Floor, Toronto, M4T 2S3, Ontario, Canada

Abstract

The quality of cold sprayed copper coatings in the as-sprayed condition heavily relies on the characteristics of the feedstock powder. While previous studies have delved into the influence of particle velocity, size, and surface oxides on the quality of as-sprayed coatings, little attention has been paid to investigating the heat treatment responses of coatings with distinct initial characteristics. In previous work, the effects of particle velocity, size, and surface oxides on as-sprayed coating properties (i.e microstructural characteristics, mechanical properties and electrical conductivity) were investigated. Coatings with different as-sprayed quality were produced, ranked from “best” to “worst” as follows: Fine-4.9, Coarse-4.9 and Fine-2.1. The differences in properties were attributed to variations in the amounts of defects at the particle-particle interfaces (PPIs), caused by different process parameters (i.e gas pressure) and powder characteristics (i.e particle size) for each coating. The present study focuses on the subsequent

heat treatment of these coatings under identical conditions (1 hour at 350 °C, under ambient atmosphere), to monitor the evolution of their microstructural characteristics, mechanical and electrical properties. The results show that in all cases, the ductility and electrical conductivity of the coatings generally improved with heat treatment. This is primarily attributed to the redistribution of surface oxides at the PPIs that improved the bonding between the particles. However, the bonding between the particles and properties of the Coarse-4.9 did not improve up to the levels of the Fine-4.9 and Fine-2.1, even though the latter exhibited much inferior properties in the as-sprayed condition. Microstructural analysis of the surface oxides at the PPIs of the, as-sprayed, Coarse-4.9, suggest that their higher thickness versus the other two coatings may have contributed to the retardation of sintering in that case. Finally, a correlation between the ductility, electrical conductivity and 3-D defect areal fraction for the heat-treated coatings is established.

1. Introduction

Cold spraying has emerged as a promising technique for depositing copper onto carbon steel surfaces [13]. In one example application, cold sprayed copper coatings are being considered for the corrosion protection of used nuclear fuel containers in a Deep Geological Repository (DGR) [2]. Unlike conventional thermal spray methods, cold spraying offers distinct advantages such as the fabrication of dense coatings devoid of open porosity and exhibiting high strength.

Nevertheless, a notable drawback of the cold spray process lies in the extreme brittleness of coatings in the as-sprayed (AS) condition. This brittleness primarily stems from the presence of defects due to poor interparticle bonding, as well as work hardening during deposition. In the case of cold sprayed copper, tensile elongation is nearly zero in the as-sprayed state [4] [7].

Moreover, the electrical conductivity of the coatings is lower compared to bulk copper, as the presence of defects in the microstructure is known to hinder electron transport.

Heat treatments at relatively low temperatures are commonly employed to address this issue.

Such treatments facilitate sintering of weakly bonded particle-particle interfaces (PPIs) by break-up and then coarsening of entrapped oxides, resulting in improved ductility. For example, heat treatment at 350 °C for 1 hour has been reported to increase the tensile ductility from near-zero to over 20% [5, 6]. Concurrently, recovery and recrystallization processes occur, leading to the annihilation of dislocations and the formation of equiaxed grains [6].

Examples of the effect of heat treatment on the properties of cold sprayed copper coatings are presented in Table 1.

Table 1: Data from the cold spray literature on the evolution of properties of copper coatings (AS=as sprayed and HT = Heat-Treated).

Reference	Spray parameters	Condition	Tensile Strength (MPa)	Ductility	Electrical conductivity (IACS)	Porosity
[7]	Gas pressure and temperature: 3 MPa - 305 °C	AS	46	<0.1%	-	-
	Gas species: Nitrogen (“low” particle velocity) Particle size range: 5-25 µm	HT 400°C, 1h	171	0.51%	-	-
	Gas pressure and temperature: 2.5 MPa -305 °C	AS	453	1.92%	-	-
	Gas species: Helium (“high” particle velocity) Particle size range: 5-25 µm	HT400°C, 1h	278	20.99%	-	-
[9]	Gas pressure and temperature: 1.4 MPa – 300 °C	AS	-	-	7.07%	~0.8%
	Gas species: Air Particle velocity: 455 m/s Particle size range: 10-45 µm	HT300°C, 1h	-	-	34%	~0.4%
	Gas pressure and temperature: 2.2 MPa - 450 °C	AS	-	-	33%	~0.3%
	Gas species: Air Particle velocity: 537 m/s Particle size range: 10-45 µm	HT300°C, 1h	-	-	78.45%	~0.1%
[5, 6]	Gas pressure and temperature: 4.9 MPa – 800 °C	AS	171	0.2%	69%	0.32%
	Gas species: Nitrogen Particle velocity: ~550–750 m/s Particle size range: 21-55 µm	HT350°C, 1h	200	23%	90.7%	0.3%
		HT600°C, 1h	195	27%	-	0.3%
[17]	Gas pressure and temperature: 3 MPa – 305 °C	AS	-	-	61.58%	-
	Gas species: Nitrogen Particle velocity: No data Particle size range: 5-25 µm	HT200°C, 1h	-	-	74.96%	-
		HT400°C, 1h	-	-	86.21%	-
		HT600°C, 1h	-	-	90.74%	-
[10]	Gas pressure and temperature: 2 MPa – 150 °C -	AS	-	-	45.37%	-
	Gas species: Nitrogen Particle velocity: No data Particle size range: 11.2-41.6 µm	HT650°C, 12h	-	-	~95%	-

The studies of Tam et al. (2022) [5,6], Stoltenhoff et al. (2006) [17] and Li et al (2006) [10], showed that the electrical conductivity and ductility of cold sprayed copper coatings can be significantly increased with heat treatment. It was also shown that the magnitude of the improvement in those properties increases with the heat treatment temperature.

However, it has been noted that even minor variations in feedstock powder characteristics or process parameters can significantly influence the response of the coating to heat treatment. For instance, the addition of Al and Si impurities at levels in the hundreds of ppm to pure copper powder can reduce tensile ductility of the coatings, even following heat treatment, from 23% to 8% [11]. As shown in Table 1 researchers have observed that coatings sprayed with helium exhibit notably higher ductility after identical heat treatments compared to those sprayed with nitrogen [7]. It was also shown that the evolution of tensile strength for the cold sprayed coatings with heat treatment seems to follow different trends, depending on the spray conditions. Coatings sprayed with helium as the carrier gas, which is known to increase the particle velocity, resulted in exceptionally high tensile strength values compared to coatings sprayed under nitrogen. After being subjected to the same heat treatment, the He-sprayed coatings experienced a decrease in the tensile strength. This contrasts with the initially low tensile strength nitrogen-sprayed coatings which increased after heat treatment [7].

Moreover, the findings of [7] and [9] reveal another observation regarding the evolution of the ductility and electrical conductivity with heat treatment in that the resulting properties of the heat-treated coatings strongly depend on the respective spray condition. Namely, coatings that possessed greater as-sprayed ductility [7] or electrical conductivity [9] than others reached higher values in those properties after being subjected to the same heat treatment.

The above observations are related to the fact that coatings sprayed at higher particle velocity (i.e. coatings sprayed under helium), had better interparticle bonding in the as-sprayed condition and therefore, a lower amount of defects at the PPIs compared to those sprayed under nitrogen. Defects can act as crack initiation sites during mechanical loading, which explains the superior as-sprayed ductility of helium-sprayed coatings. During heat treatment, diffusion-driven processes, such as recrystallization and spheroidization of defects take place, resulting in a further decrease in the amount of crack-initiation sites [7]. In the case of helium-sprayed coatings, heat treatment (HT 400°C, 1h) reduced the amount sufficiently, as the ductility increased above 20% [7]. On the contrary, in the case of nitrogen-sprayed coatings, heat treatment under the same conditions did not sufficiently reduce the amount of defects at the PPIs, resulting in only a minimal improvement in ductility [7].

Similar claims were made to justify the different magnitudes of improvement on the electrical conductivity values of cold sprayed copper coatings with different as-sprayed states, after heat treatment at the same conditions, by Phani et al. (2007) [9].

In this study, the effect of particle size on post-heat treatment characteristics are investigated by producing three cold-sprayed copper coatings with different as-sprayed conditions, generated by variations in particle sizes and particle velocities. To explore the impact of these parameters on heat-treatment response, the coatings are subjected to identical heat treatment conditions.

2. Experimental Procedure

Three distinct cold-sprayed copper coatings, denoted as Fine-4.9, Coarse-4.9, and Fine-2.1. were produced. The nomenclature reflects both the feedstock powder size utilized in the production of

each coating, fine ($d_{50} = 29.53 \mu\text{m}$) and coarse ($d_{50} = 68.67 \mu\text{m}$), and the gas pressure applied during cold spraying (4.9 MPa and 2.1 MPa). By imposing variations in feedstock powder characteristics and process parameters, different microstructural characteristics, mechanical, and physical properties are anticipated. A comprehensive analysis of the as-sprayed characteristics of these coatings has been reported in a previous paper [20].

The heat treatments were conducted in a box furnace at 350°C for a duration of 1 hour under ambient atmosphere. This heat treatment was selected based on previous work to obtain the desired ductility ($\sim 20\%$) [5, 11]. Alumina crucibles were employed to contain the samples, ensuring they were in direct contact with the thermocouple used for temperature measurement. The samples were placed in the furnace at room temperature and then heated to 350°C at a controlled heating rate of $10^{\circ}\text{C}/\text{min}$. Once the desired temperature was attained, the samples were held within the furnace for 1 hour. Following this, the furnace was powered off, and the samples were allowed to cool in the furnace with the door open until reaching room temperature. Henceforth, the samples examined in this study are labelled as Fine-4.9-HT350, Coarse-4.9-HT350 and Fine-2.1-HT350.

Following the heat treatment, the visible surface oxide was removed with the use of a 1200 grit grinding paper. Then a precision saw was used to extract small rectangular samples from the cross section of each coating, parallel to the traverse direction of the cold spray gun. These samples were then used for microstructural characterization, mechanical and electrical resistivity testing.

2.1 Microstructural Characterization

One rectangular sample from each coating was used for microstructural observation. Initially, each sample was cold mounted by using Clarocit powder and hardener liquid. After curing for 2 hours, the surface of the sample was progressively polished using 1200 grit grinding paper, and 3 μm and 1 μm diamond suspensions. The samples received an additional polishing by using a colloidal silica suspension (0.02 μm) in a vibratory polisher.

The microstructures of the polished cross sections were observed in a Clemex Optical Microscope, and a Hitachi SU-8230 Scanning Electron Microscope. Prior to microscopic observation, the samples were coated with a one nanometer-thick layer of carbon.

2.2 Mechanical Properties

The mechanical properties of the three coatings (Fine-4.9-HT350, Coarse-4.9-HT350 and Fine-2.1-HT350) were evaluated by performing Shear Punch Tests (SPTs). The punch was moving at a constant speed of 1.2 mm/min, and the maximum detectable load was 100 kN. The average clearance between the punch and the die, r_{avg} , was 0.8875 mm. The dimensions of the samples were about 0.5 cm in width and length, while the thicknesses in all cases were in the range of 1.2-1.7 mm. Five specimens from each coating were tested, to obtain the respective average Shear Yield Strength (SYS), Ultimate Shear Strength (USS) and effective ductility (ϵ_{eff}) values [20, 29, 30].

2.3 Electrical Resistivity

The samples used for microstructural characterization were also used for electrical resistivity testing. Initially, the three mounted samples were placed in acetone for 48 hours in order to be released from their mounts. They were then slowly ground by using 600 and 1200 grit SiC

grinding papers to acquire the desired dimensions (length, width and thickness) for the test. For the Fine-4.9-HT350 sample, the final dimensions were 6 x 2 mm and the final thickness 550 μm . For the Coarse-4.9-HT350, the final dimensions were 6 x 6 mm and the final thickness was 760 μm . For the Fine-2.1-HT350 the final dimensions were 6 x 6 mm and the final thickness 465 μm .

The electrical resistivity was measured by the 4-point probe technique, by applying the same methodology as in our previous work. The applied currents used for the measurements of all coatings were in the ranges of 150-290 mA. The average resistivity values were calculated by the following formula:

$$\rho = \frac{V}{I} t F C$$

Where, t is the thickness of the sample in μm , V is the voltage measured by the multimeter in mV, I is the current applied on the sample by the power source in mA. F and C are fitting parameters that depend on the geometry of the sample. The “F” factor depends on the ratio of sample thickness to probe spacing and the “C” factor on the ratio of the sample width to probe spacing and the length to width ratio. In this case, the F and C factors were determined to be 2.45 and 1, respectively, for both the Fine-2.1-HT350 and Coarse-4.9-HT350 coatings. For the Fine-4.9-HT350 coating, the F and C factors were determined to be 1.24 and 1, respectively [8].

3. Results

3.1 Microstructure

Figure 1 presents the results from the defect observations of the three coatings using the optical microscope. For each coating, the area fraction of all three-dimensional (3-D) defects was

determined. A comparison between the average 3-D defect areal fraction values in the AS and HT350 conditions is presented in Fig. 2.

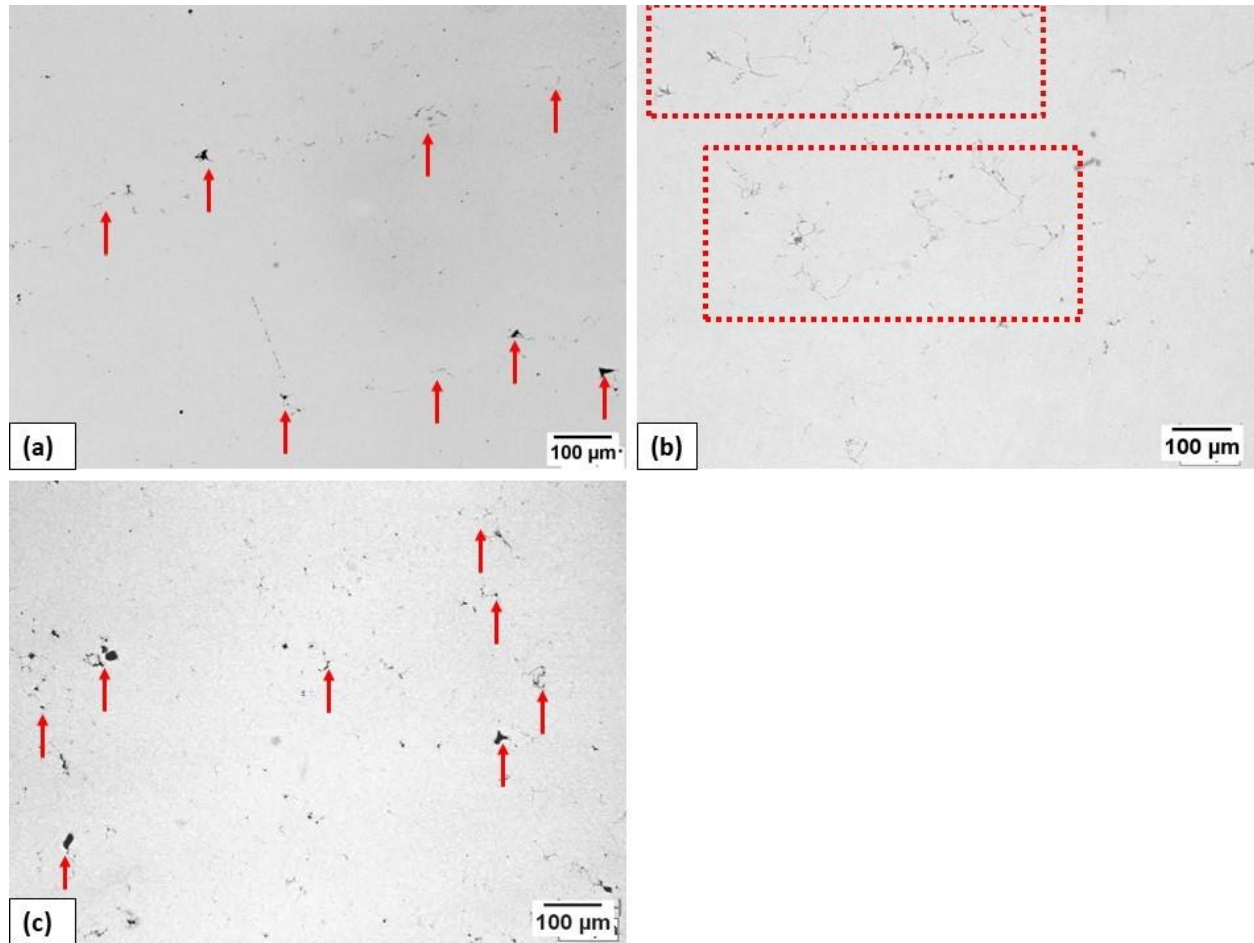


Figure 1: Optical microscope images of the polished cross sections at the 100X magnification – (a) Fine-4.9-HT350, (b) Coarse-4.9-HT350, (c) Fine-2.1 HT350 coating.

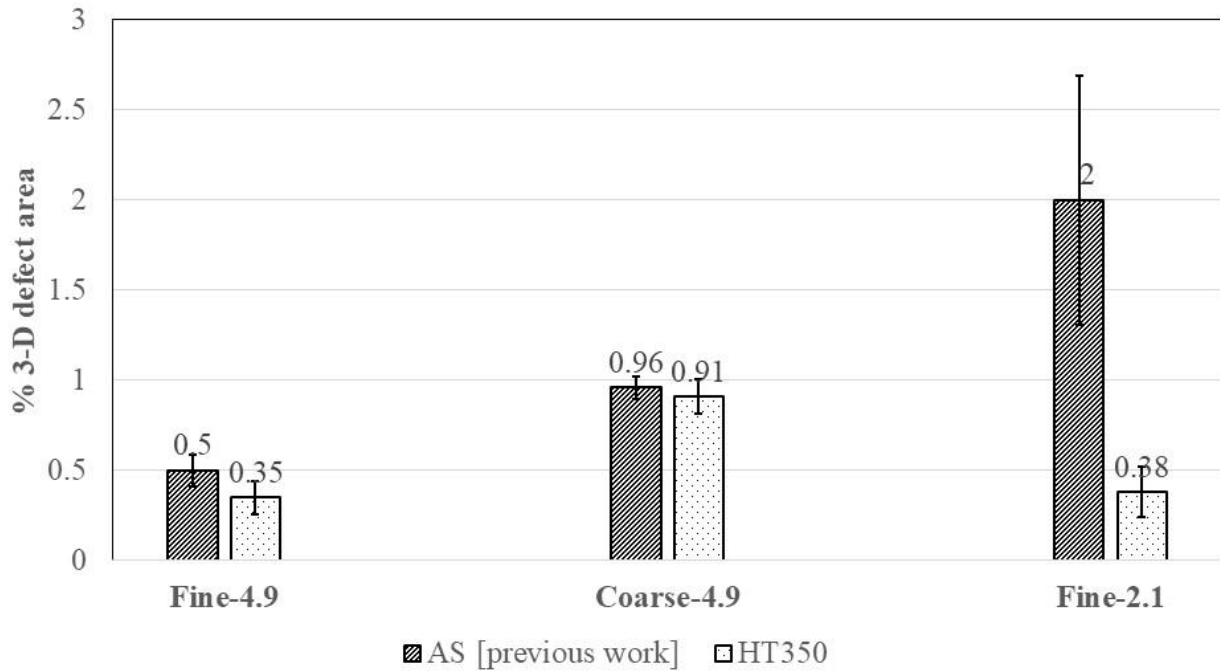


Figure 2: Comparison of the 3-D defect areal fraction of the three coatings before and after heat treatment. The values in the AS coatings were taken from previous work [20]

In the case of the Fine-4.9-HT350 coating, the 3-D defects are localized within regions parallel to the transverse direction of the cold spray gun during spraying. They appear slightly less continuous compared to the as-sprayed condition (shown in previous work). A limited number of isolated micron-sized pores are also observed. Those pores appear to be slightly coarser compared to the AS condition. Overall, the average 3-D defect areal fraction is reduced from 0.5% to 0.35%, after heat treatment (Fig. 2). In the Fine-2.1-HT350 coating case, the presence of 3-D defects and micron size pores are comparable to that of the Fine-4.9-HT350 coating with average values of 0.35% and 0.38%, respectively. Specifically for the Fine-2.1 coating, a significant decrease in 3-D defect areal fraction was observed considering the initial as-sprayed average value of 2%.

In contrast, the Coarse-4.9 coating did not exhibit the same level of reduction in 3-D defects. Continuous, interconnected particle-particle defects can be observed in the microstructure of the coating at a higher frequency compared to the other two cases. In fact, only a very small reduction in 3-D defect areal fraction was observed, i.e. from 0.96% to 0.91% for the as-sprayed and heat-treated conditions, respectively.

To investigate the morphology and appearance of the 3-D defects, the polished cross sections of the samples were also examined with an SEM microscope using the ECCI mode. The results are presented in Figs. 3-6. Fig. 3 presents the microstructures of the coatings at low magnification.

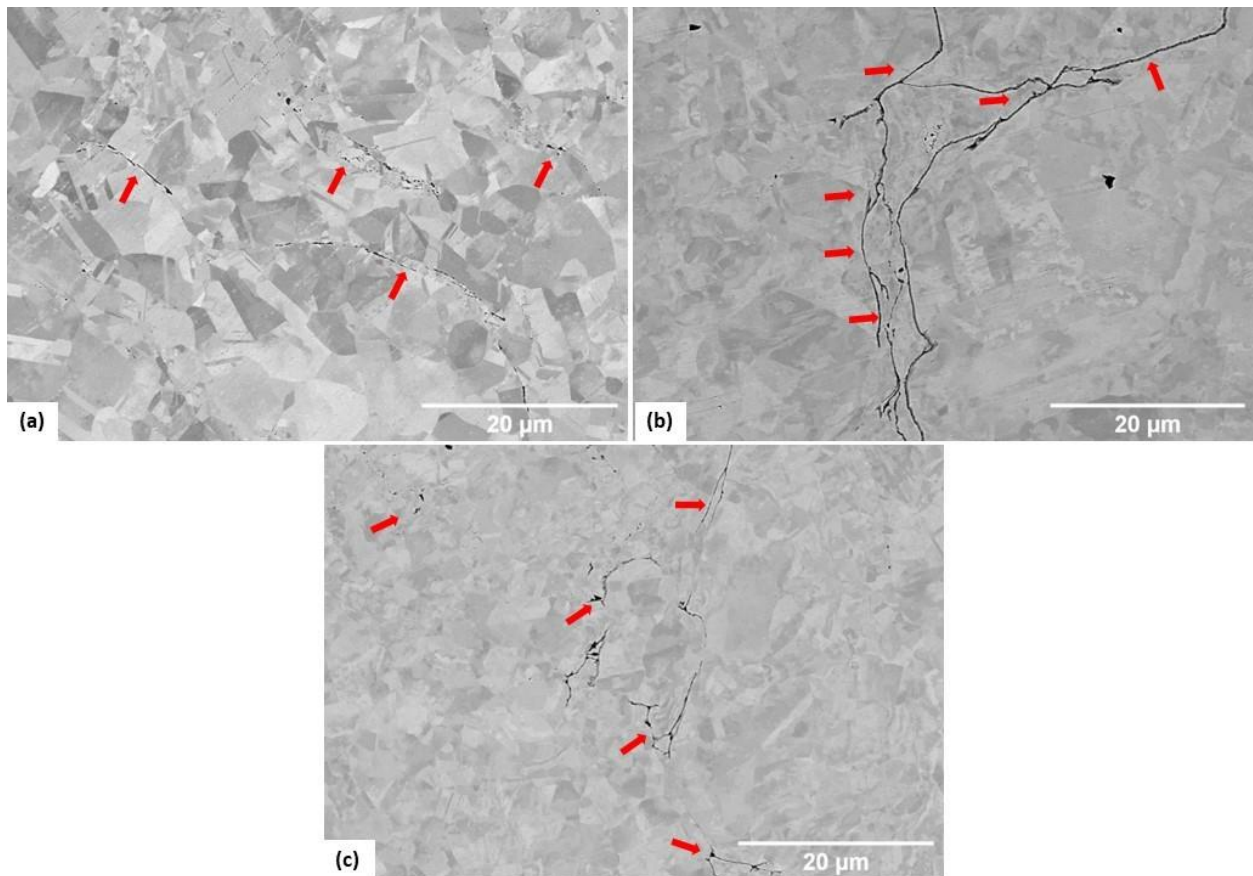


Figure 3:(a) Fine-4.9-HT350 coating, (b) Coarse-4.9-HT350 coating and (c) Fine-2.1-HT350 coating.

From the low magnification the SEM micrographs, the defect areal fraction values were estimated to be 0.25% for the Fine-4.9, 0.98% for the Coarse-4.9, and 0.3% in the Fine-2.1, which are in accord with the results from the optical microscope images.

Moreover, large numbers of interconnected PPIs (arrowed) were seen in the Coarse 4.9, while in both the Fine coatings, the corresponding connected PPIs are much shorter in length and less numerous. At high magnification, the defects appear to be oxide films. Morphological evolution of these films with heat treatment is illustrated in images (Figs. 4-6).

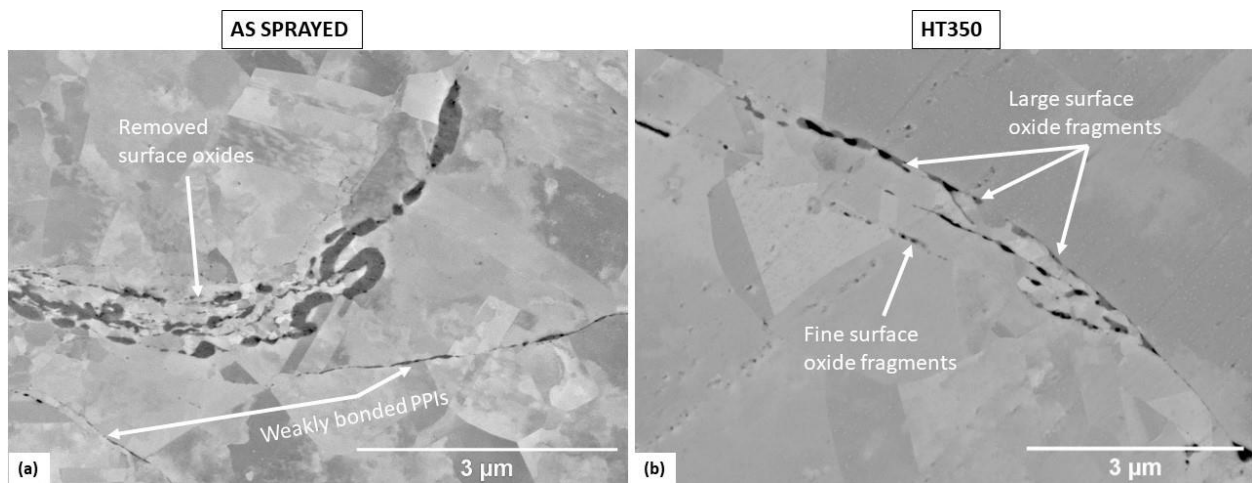


Figure 4: High magnification ECCI micrographs for the Fine-4.9 coating – (a) surface oxides and 3-D defects in the as-sprayed condition (same image was used in previous work [20]0), (b) surface oxides and 3-D defects after heat treatment.

For the Fine-4.9 coating, an image from previous work (Fig. 4a) shows the surface oxide fragments (arrowed dark grey contrast regions), to be dispersed into the copper matrix by viscous flow. A small amount thin surface oxides still intact at the PPIs is also indicated (Fig. 4a). After heat treatment (Fig. 4b), the incidence of surface oxide fragments is greatly reduced and redistributed in the copper matrix. The thin, continuous films seem to be somewhat fragmented and spheroidized. Furthermore, grain growth is also observed after heat treatment; after heat

treatment, the size of the copper grains at the interior of sprayed particles, surrounding the surface oxides (Fig. 4b) is larger and their appearance more equiaxed compared to the as-sprayed condition (Fig. 4a).

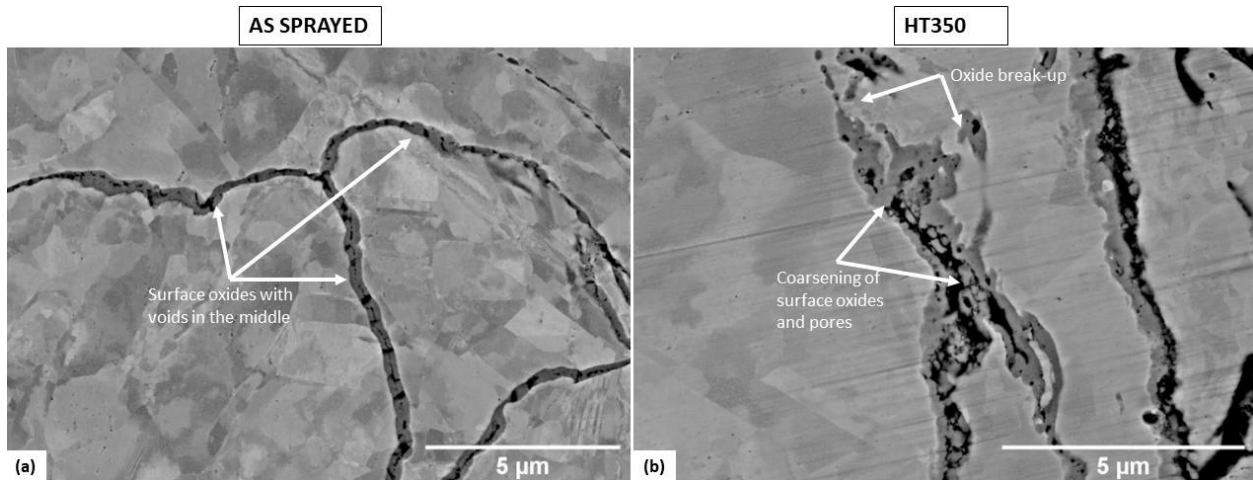


Figure 5: High magnification ECCI micrographs for the Coarse-4.9 coating – (a) 3-D defects from the Coarse-4.9 coating in the as-sprayed condition (same image was used in previous work [20]), (b) 3-D defects in the Coarse-4.9-HT350 coating.

For the Coarse-4.9 coating, our previous work showed that the 3-D defects (indicated by the arrows in Fig. 5a) consist of thick continuous surface oxide layers that are adjacent to the PPIs. Thin interconnected voids also exist between the surface oxides.

After heat treatment, coarsening of the surface oxide layers is observed. They appear to be much thicker, with a wavier appearance. The voids between the surface oxides also appear to be thicker compared to the as-sprayed condition. Promotion of bonding between interfaces can also be observed, to a limited extent. In some limited regions, oxide coarsening resulted in break-up, and the appearance of copper bridges between the two particles. Nevertheless, bonding is still prohibited by thick surface oxides and voids in a large part of the region.

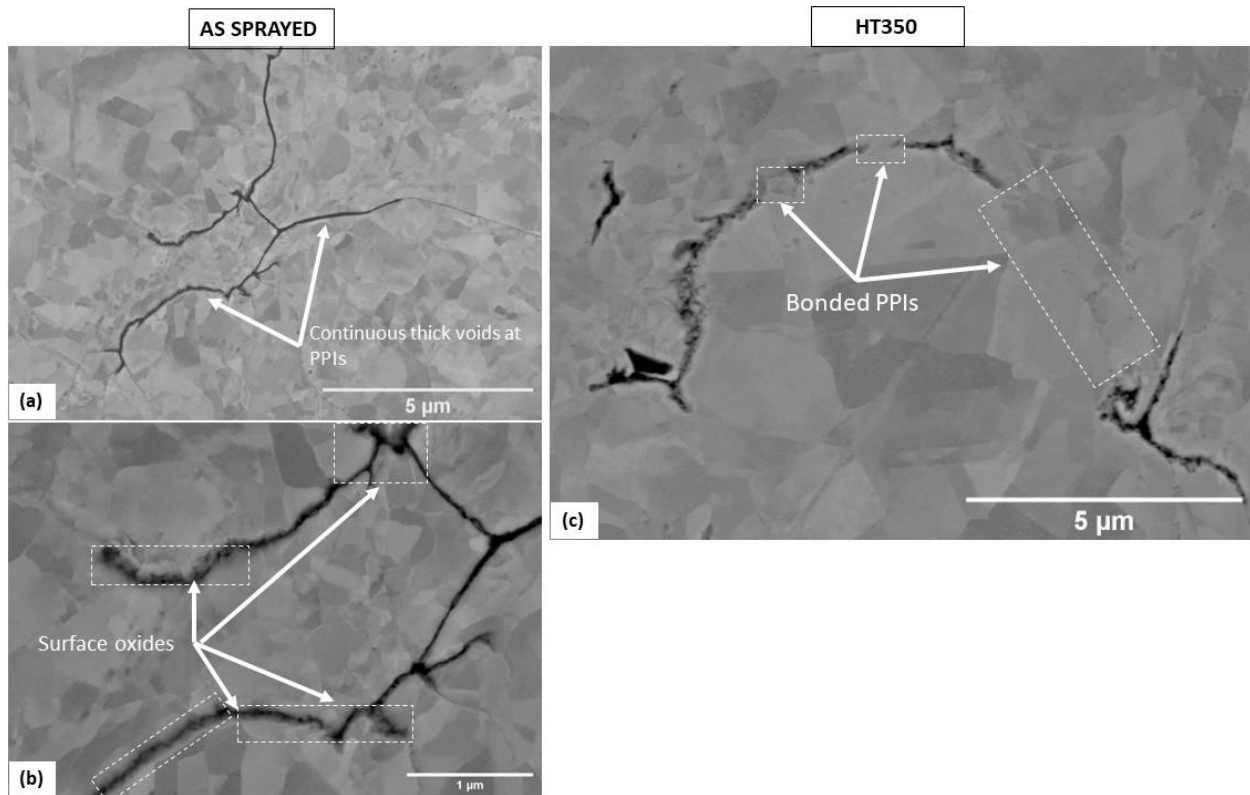


Figure 6: High magnification ECCI micrographs for the Fine-2.1 coating – (a) & (b) 3-D defects from the Fine-2.1 coating in the as-sprayed condition, (c) 3-D defects in the Fine-2.1-HT350 coating.

In the Fine-2.1 coating case in the AS condition the PPIs consist of long thick continuous voids (Fig. 6a), followed by thin surface oxide films adjacent to the interfaces, revealed at higher magnification (Fig. 6b).

After heat treatment (Fig. 6b), the surface oxide films seem to occupy the regions that previously consisted of voids, and the voids became thinner and less continuous. It appears that the thin oxide films that were previously adjacent to the surfaces of the particles have sintered together with heat treatment. Also, copper bridges at the PPIs are observed, indicating healing of the weakly bonded interfaces by promotion of metallurgical bonding.

Changes in the interior grain structure of the sprayed particles were also observed in the Coarse-4.9-HT350 and Fine-2.1-HT350 cases; the grains inside each particle appear to be more equiaxed compared to their respective as-sprayed microstructures. However, in contrast with the Fine-4.9-HT350, no significant grain growth was observed in those two cases.

It is noted that in all three cases (Figs 4-6), EDS mapping analysis (not shown here) confirmed that the dark grey phases were rich in oxygen and relatively poor in copper, confirming that these phases are copper oxides.

3.2 Mechanical and Electrical Properties

In previous work [20], the electrical resistivity of the Fine-4.9, Coarse-4.9 and Fine-2.1 coatings was measured by using the 4-point probe method. The USS and ε_{eff} were also evaluated by performing SPTs. Fig. 7 shows the results on the evolution of those properties with heat treatment.

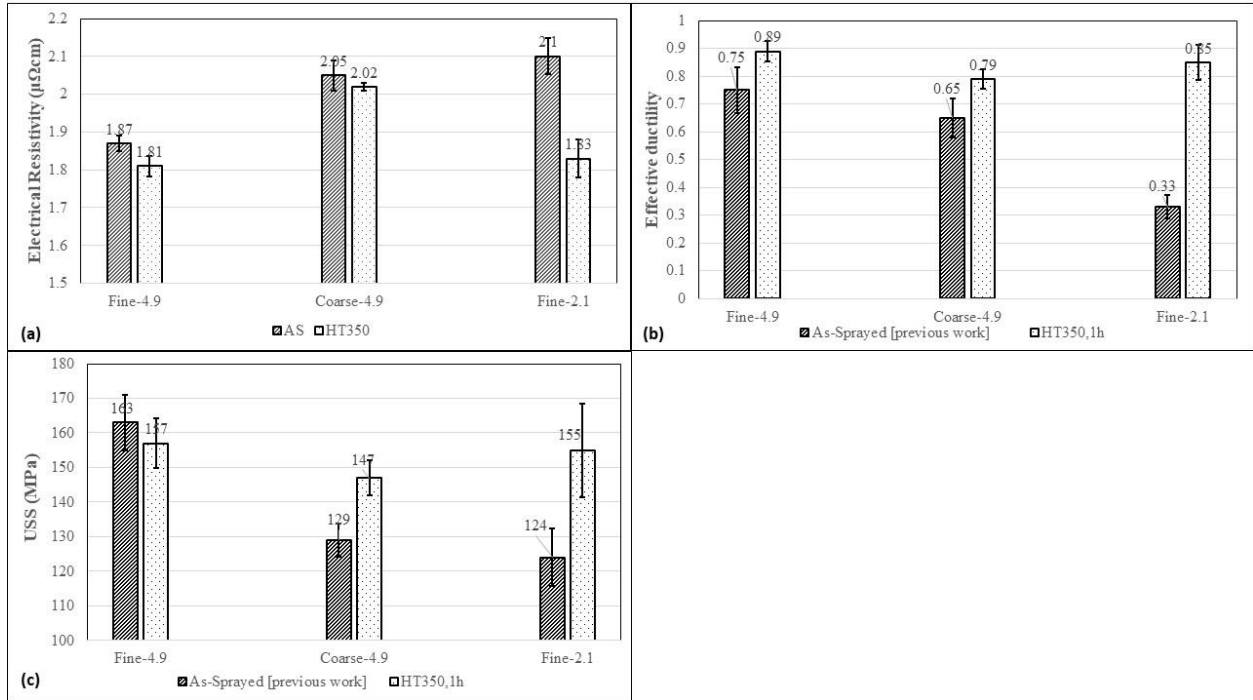


Figure 7: (a) Average electrical resistivity of the three coatings for the as-sprayed [20] and heat-treated conditions, (b) Average effective ductility (ϵ_{eff}) of the three coatings for the as-sprayed [20] and heat-treated conditions, (c) Average Ultimate Shear Strength of the three coatings in the as-sprayed [20] and heat-treated condition.

The electrical resistivities of the Fine-4.9-HT350 and Fine-2.1-HT350 coatings were at similar levels, i.e., $1.81 \mu\Omega \text{ cm}$ (95.3% IACS) and $1.83 \mu\Omega \text{ cm}$ (92.2% IACS), respectively.

The case was the same regarding their respective effective ductility (ϵ_{eff}) values, i.e., 0.89 for the Fine-4.9HT350 and at 0.85 for the Fine-2.1HT350. Both coatings exhibited improvement compared to their respective as-sprayed values, especially the Fine-2.1, which in comparison had much lower ductility and higher resistivity in the as-sprayed condition.

In the case of the Coarse-4.9-HT350 coating, although a slight improvement was noted in ductility after heat treatment from to 0.79, it remained lower compared to Fine-4.9-HT350 and Fine-2.1-HT350. Similarly, the electrical resistivity of the Coarse-4.9-HT350 decreased only

slightly with heat treatment, from 2.05 $\mu\Omega$ cm (84.1% IACS) to 2.02 $\mu\Omega$ cm (85.35% IACS). Furthermore, the evolution of the USS with heat treatment exhibited different trends from one coating to another. In the Fine-4.9-HT350 coating case, the average USS decreased slightly from 163 MPa to 157 MPa. In contrast, the USS in both the Coarse-4.9-HT350 and Fine-2.1-HT350 coatings increased significantly. The increase for the Coarse-4.9-HT350 was from 129 MPa to 147 MPa, and for the Fine-2.1-HT350 from 124 MPa to 155 MPa.

4. Discussion

It is well established in the cold spray literature that weakly bonded PPIs act as crack initiation sites during mechanical loading, reducing the ductility and mechanical strength of the coatings [24, 25]. Furthermore, it is known from Matthiessen's rule that internal defects in metallic materials will act as scattering centers for electrons, hindering their mobility and increasing the electrical resistivity [22, 23]. For the case of cold sprayed copper, earlier works reported that increasing the amount of entrapped surface oxides at the PPIs will result in an increase of the interface resistance between the sprayed particles [24, 25], elevating the electrical resistivity of the coating [24, 25].

In agreement with the above, in both as-sprayed [20] and heat-treated conditions, the electrical conductivity/resistivity and ductility of each coating correlate with its respective 3-D defect areal fraction (Figs. 2 and 7). Coatings with relatively low 3-D defect areal fraction exhibit higher ductility and lower electrical resistivity compared to others with higher fractions. Therefore, the discussion will focus on the evolution of 3-D defect areal fraction in the three coatings for both the as-sprayed and heat-treated conditions.

4.1 As-Sprayed

As shown in previous work [20], due to the relatively high particle velocity, the Fine-4.9 coating exhibited the best properties in the as-sprayed condition. In terms of entrapped surface oxide characteristics, a large amount of surface oxides was removed from the PPIs to the interior of the sprayed copper particles. This is likely caused by a fragmentation-melting-viscous flow mechanism, which allowed for metallurgical bonding to occur in a significant areal fraction of the PPIs. Only a limited amount of thin, non-continuous surface oxides remained adhered to the particle boundaries (Fig. 4a). As a result, this coating exhibited the highest electrical conductivity and ductility in the as-sprayed condition. The ultimate shear strength was also relatively high [20].

The other two coatings (i.e., Coarse-4.9 and Fine-2.1) are similar in the sense that the surface oxides remained intact to the PPIs, with no evidence of removal by melting and viscous flow. However, in the Coarse-4.9 case, the oxides are less continuous, thicker, and are located mainly at the edges of the sprayed particles when compared to the Fine-2.1. Thin continuous voids are also located between the surface oxides of two contacting particles. In contrast, in the Fine-2.1 case, thin surface oxides are intact at the whole periphery to the particles, preventing metallurgical bonding and resulting in the formation of a network of defects, which is much more continuous compared to the Coarse-4.9. Both coatings exhibited inferior ductility and electrical conductivity compared to the Fine-4.9 (Fig. 7), especially in the Fine-2.1 case. The latter was attributed to the higher 3-D defect areal fraction of the Fine-2.1 compared to the Coarse-4.9 (Fig. 2).

The lower amount of 3-D defects of the Coarse-4.9 compared to the Fine-2.1 was attributed to the higher η ratio that was achieved during the spraying of the former (i.e., Coarse-4.9). The two coatings were sprayed at similar particle velocities (556 m/s and 566 m/s for the Coarse 4.9 and Fine-2.1, respectively) but in the Coarse-4.9 case the used feedstock powder had a larger average particle size, and therefore lower critical velocity compared to the Fine-2.1 [20].

The average USS values of the Fine 2.1 and Coarse 4.9 were similar with each other (124 MPa and 129 MPa, respectively), but lower compared to the Fine-4.9 (163 MPa). Since the Coarse-4.9 and Fine-2.1 coatings exhibited different 3-D defect areal fractions between each other, the USS differences can be rationalized on the basis of work hardening differences. The high particle velocity in the Fine-4.9 case led to higher work hardening and USS values for the coating, compared the Fine-2.1 and Coarse-4.9. The superior interparticle bonding of the former may have also contributed to the high USS, however the current study suggests that it is more sensitive to the work hardening during deposition [20].

4.2 Heat-Treated

Heat treatment appears to generally reduce the 3-D defect areal fraction of each coating, resulting in an increase on its respective ductility and a decrease on its respective electrical resistivity. However, the reduction of the 3-D defect areal fraction and the resulting changes in ductility and resistivity were not the same for all the coatings (Fig 2). The Fine-4.9-HT350, which had the lowest 3-D defect areal fraction in the as-sprayed condition (0.5 %), exhibited the lowest amount post-heat treatment (0.35%). In the Coarse-4.9-HT350 case, where the amount of defects was higher in the as-sprayed condition (0.96%), the reduction post heat treatment was not significant. Notably, although the Fine-2.1 coating exhibited the highest amount of 3-D defects

in the as-sprayed condition (~2%) overall, their areal fraction was significantly reduced post-heat treatment well below the levels of the Coarse-4.9-HT350, approaching the value of the Fine-4.9-HT350. With respect to the reduction in 3-D defects, the ductility and resistivity were also improved, exceeding the respective values of the Coarse-4.9-HT350 and being slightly below the Fine-4.9-HT350 (Fig. 7).

As discussed in the introduction section, the data from the cold spray literature (Table 1) suggests that, although heat-treatment would generally improve the characteristics of the coatings, those with superior features in the as-sprayed condition will remain superior after heat treatment. The present work suggests that this claim may not be necessarily true. That is, while the Fine-2.1 coating exhibited more 3-D defects and inferior properties than the Coarse-4.9 in the as-sprayed condition, there was a significant improvement in properties for Fine-2.1-HT350 after heat treatment surpassing those of the Coarse-4.9-HT350.

4.2.1 Evolution of surface oxides with heat treatment

Since ECCI images revealed that surface oxides are entrapped at the 3-D defects of PPIs in as-sprayed coatings, the reduction of those defects through the sintering of the sprayed particles is greatly affected by the evolution of the surface oxides during heat treatment. In all cases, as shown in Figs 4-6, the surface oxides appear to have been redistributed during heat treatment, allowing for bonding between the surfaces of the sprayed copper particles. However, the nature of the redistribution differs from one coating to another.

In the Fine-4.9-HT350 case the surface oxides appear to be fragmented into nano-sized individual particles, dispersed around the PPI (Fig 4b). Their redistribution appears to have taken place following the Ostwald Ripening mechanism, according to which, coarser particles grow to

the expense of finer particles [26, 27]. Coarsening of oxide inclusions in additively manufactured (AM) metal parts by Ostwald Ripening has been reported by Deng et al. (2022) [21]. The authors reported that during the annealing of AM 316L stainless steel parts entrapped oxide inclusions grow to the expense of finer ones, by means of diffusion processes (lattice diffusion, grain boundary diffusion and dislocation pipe diffusion). They also stated that the oxide growth is facilitated by their interaction with moving grain boundaries during recrystallization and grain growth [21]. Furthermore, in a case similar with the present study, Tam et al (2021) reported that the surface oxides at the PPIs of cold sprayed copper coatings may redistribute via Ostwald Ripening during annealing, allowing bonding between the sprayed copper particles to take place [5]. Also, the fragmentation of the surface oxides was facilitated by grain boundary grooving, which occurred because of the grain growth during heat treatment [5].

Grain growth appears to have occurred in the case of the Fine-4.9-HT350 coating. The high particle velocity during cold spraying may have introduced a larger amount of dislocations [20], and therefore more driving force for the nucleation and growth of recrystallized grains during heat treatment. Therefore, for this particular coating, it is proposed that grain growth facilitated the oxide redistribution resulting in a significant improvement in the bonding, ductility and electrical resistivity. These properties were superior in the Fine-4.9-HT350, compared to the other two coatings. Grain growth and Ostwald ripening did not seem to occur in the Fine-2.1-HT350 case, however bonding between the copper particles was significantly improved compared to the as-sprayed condition, approaching the levels of the Fine-4.9-HT350. Similarly, the ductility and electrical resistivity of the Fine-2.1-HT350 reached similar levels.

Evidence of surface oxide diffusion and redistribution is also observed for the Coarse-4.9-HT350 coating, compared to its respective as-sprayed condition (Fig. 5). However, it appears to happen

at an earlier stage when compared to the other two cases (Fine-2.1-HT350, Fine-4.9-HT350). Nearly all of the surface oxides are still intact at the PPIs, coupled with continuous voids.

This retardation of sintering between the sprayed particles in the Coarse-4.9-HT350 coating is attributed to the higher thickness of the surface oxides at its PPIs in the as-sprayed condition, compared to the Fine-2.1 and Fine-4.9 coatings. Surface oxides are known to oppose sintering of metal powders. Studies in sintering in conventional powder metallurgy suggest that the bonding of two surfaces of metal particles is preceded by an incubation period, during which the surface oxide dissolves into the metal matrix if oxygen solubility in the metal allows [18, 19]. The ratio of oxide thickness to particle size is the deciding factor for this retardation of sintering [18] [19]. In the as-sprayed condition, the surface oxide thickness was much larger in the Coarse-4.9 case compared to the Fine-2.1. Although the total amount in terms of areal fraction was smaller (for the Coarse-4.9), it appears that the high thickness impeded its break-up and redistribution during heat treatment.

Another factor that could have facilitated the diffusion processes in the case of the Fine-2.1-HT350 and Fine-4.9-HT350 versus the Coarse-4.9-HT350 is the smaller grain size at the interior of the sprayed particles of the former two versus the latter, in the as-sprayed condition (Figs 4-6). Grain boundary diffusion is promoted in cases where the grain size is relatively small, and takes place at relatively low temperatures, similar to the heat treatment conditions in the present study [14, 28].

4.2.2 Effect of heat treatment on the Ultimate Shear Strength (USS)

It was observed that the USS of the Fine-4.9 response to heat treatment differed with those of the Fine-2.1 and Coarse-4.9. For Fine-4.9, where it was relatively high in the as-sprayed condition

(163 MPa), it decreased after heat treatment to 157 MPa. In contrast, in the latter two cases (Fine-2.1 and Coarse-4.9), where the values were lower in the as-sprayed condition (124 and 129 MPa, for the Fine-2.1 and Coarse-4.9, respectively), the USS increased with heat treatment (155 and 147 for the Fine-2.1 and Coarse-4.9, respectively).

As mentioned earlier in Section 4.1, the Fine-4.9 coating was cold sprayed at higher particle velocity (631 m/s) compared to the other two coatings (555 m/s and 566 m/s, for the Coarse-4.9 and Fine-2.1, respectively). Therefore, work hardening was more prominent in the Fine-4.9 case, resulting in more dislocations being introduced when compared to the Coarse-4.9 and Fine-2.1 cases. Since dislocations are known to be the driving force for recrystallization and grain growth, this microstructural evolution is considered to be more prominent for Fine-4.9 when compared to the Coarse-4.9 and Fine-2.1 coatings. Furthermore, the 3-D defect areal fraction of the Fine-4.9 coating was already low in the as-sprayed condition, in contrast with the other two coatings, where it was higher.

The definition of sintering, given by R. A. German is “*a thermal treatment for bonding particles into a coherent, predominantly solid structure via mass transport events than often occurs in the atomic scale. The bonding leads to improved strength and a lower system energy*” [14]. Based on that definition, it is likely that the sintering which occurred during heat treatment had a stronger effect on the USS Fine-2.1 and Coarse-4.9 coatings. This explains the increase in their USS with heat treatment, compared to their as-sprayed values. Although sintering took also place at the PPIs of the Fine-4.9 (Fig. 4), the decrease in the USS during heat treatment may be explained by the annihilation of dislocations through recrystallization, and the subsequent grain growth. This may also have had an effect on the ductility and electrical resistivity accordingly.

5. Conclusions

In this study, the influence of the as-sprayed state of cold sprayed copper coatings on their subsequent heat treatment response was investigated. Three coatings were fabricated by cold spraying feedstock powders with different particle size distributions at targeted particle velocities. The key findings are as follows:

- Consistent with previous research, a correlation was found between the ductility, electrical conductivity, and the three-dimensional defect areal fraction of the coatings.
- Heat treatment improved the interparticle bonding and, consequently, most properties of the Coarse-4.9 and Fine-2.1 coatings. This was mainly due to the respectively higher 3-D defect areal fraction and redistribution of entrapped surface oxide fragments at the PPIs through diffusion processes.
- The USS decreased for the Fine-4.9 coating post-heat treatment, while it increased for the Coarse-4.9 and Fine-2.1 coatings. For Fine-4.9, this was attributed to the as-sprayed low 3-D defect areal fraction resulting in superior bonding and high dislocation density which facilitated recovery, recrystallization, and grain growth during heat treatment.
- Despite overall improvements, the final properties (3-D defect areal fraction, ductility, electrical resistivity) did not follow the initial quality ranking, of the as-sprayed coatings. While in the as-sprayed condition the properties of the Coarse-4.9 were superior than the Fine-2.1, after heat treatment, the most significant improvement was achieved with Fine-2.1 coating, while limited improvement was obtained with the Coarse-4.9. This was due to the high surface oxide thickness (the key microstructural difference of this study) of the latter, impeding enhancement of bonding at the PPIs by sintering.

- If the coating quality were varied solely by changing cold spray process parameters (e.g., particle velocity by adjusting gas pressure), the heat-treated coating quality would likely follow the as-sprayed quality. However, changes in feedstock (e.g., particle size and surface oxide thickness) can lead to microstructural differences that respond differently to heat treatment.

Future research should focus on: a) quantifying the surface oxide thickness of the feedstock powders used for the coatings, b) conducting dynamic analysis of the diffusion mechanism of entrapped surface oxides at the PPIs during heat treatment, possibly using hot stage scanning electron microscopy and, c) investigating the effect of different surface oxide thicknesses on heat treatment response, using coatings produced from powders of similar sizes to isolate particle size effects.

6. References

- [1] A. Papyrin, V. Kosarev, S. Klinkov, A. Alkhimov, V. Fomin, “Cold Spray Technology”, Elsevier, 1st Edition, 2006
- [2] P. G. Keech, P. Vo, S. Ramamurthy, J. Chen, R. Jacklin, D. W. Shoesmith (2014), “Design and development of copper coatings for long term storage of used nuclear fuel”, Corrosion Engineering, Science and Technology, 49:6, 425-430
- [3] Christopher H. Boyle, Shaker A. Meguid, “Mechanical performance of integrally bonded copper coatings for the long term disposal of used nuclear fuel”, Nuclear Engineering and Design 293 (2015) 403–412

- [4] Calla, E., McCartney, D.G. & Shipway, P.H. Effect of deposition conditions on the properties and annealing behavior of cold-sprayed copper. *J Therm Spray Tech* 15, 255–262 (2006).
<https://doi.org/10.1361/105996306X108192>
- [5] Jason Tam, Bosco Yu, Weiwei Li, Dominique Poirier, Jean-Gabriel Legoux, Jason D. Giallonardo, Jane Howe, Uwe Erb, "The effect of annealing on trapped copper oxides in particle particle interfaces of cold-sprayed Cu coatings", *Scripta Materialia*, Volume 208, 1 February 2022, 114333 <https://doi.org/10.1016/j.scriptamat.2021.114333>
- [6] B. Yu, J. Tam, W. Li, H.J. Cho, J.-G. Legoux, D. Poirier, J.D. Giallonardo, U. Erb, "Microstructural and bulk properties evolution of cold-sprayed copper coatings after low temperature annealing", *Materialia* 7 (2019) 100356 <https://doi.org/10.1016/j.mtla.2019.100356>
- [7] F. Gärtner, T. Stoltenhoff, J. Voyer, H. Kreye, S. Riekehr, M. Koçak, "Mechanical properties of cold-sprayed and thermally sprayed copper coatings", *Surface Coatings Technology* 200 (2006) 6770–6782
- [8] F. M. Smits, "Measurement of sheet resistivities with the Four-Point Probe", *The Bell System Technical Journal*, 711-716, 1958
- [9] P. Sudharshan Phani, D. Srinivasa Rao, S.V. Joshi, and G. Sundararajan, "Effect of Process Parameters and Heat Treatments on Properties of Cold Sprayed Copper Coatings", *Journal of Thermal Spray Technology*, 16, 425-434, 2007
- [10] Wen-Ya Li, Chang-Jiu Li, and Hanlin Liao, "Effect of Annealing Treatment on the Microstructure and Properties of Cold-Sprayed Cu Coating", *Journal of Thermal Spray Technology*, Volume 15(2), 206-211 (2006)

- [11] Bruno Guerreiro, Phuong Vo, Dominique Poirier, Jean-Gabriel Legoux, Xuan Zhang, Jason D. Giallonardo, "Factors Affecting the Ductility of Cold-Sprayed Copper Coatings", *J Therm Spray Tech* (2020) 29:630–641
- [12] Weiwei Li, Bosco Yu, Jason Tam, Jason D. Giallonardo, David Doyle, Dominique Poirier, Jean-Gabriel Legoux, Peter Lin, Gino Palumbo, Uwe Erb, "Microstructural characterization of copper coatings in development for application to used nuclear fuel containers", *Journal of Nuclear Materials*, Volume 532, 15 April 2020, 152039
- [13] Christopher H. Boyle, Shaker A. Meguid, "Mechanical performance of integrally bonded copper coatings for the long term disposal of used nuclear fuel", *Nuclear Engineering and Design*, Volume 293, November 2015, Pages 403-412
- [14] Randall M. German, "Sintering Theory and Practice", John Wiley & Sons, Inc, 1996
- [15] R.C. McCune, W.T. Donlon, O.O. Popoola, and E.L. Cartwright, Characterization of Copper Layers Produced by Cold Gas-Dynamic Spraying, *J. Therm. Spray Technol.*, 2000, 9(1), p 73-82
- [16] C. Borchers, F. Gärtner, T. Stoltenhoff, H. Assadi, and H. Kreye, Microstructural and Macroscopic Properties of Cold Sprayed Copper Coatings, *J. Appl. Phy.*, 2003, 93(12), p 10064-10070
- [17] T. Stoltenhoff, C. Borchers, F. Gärtner, H. Kreye, "Microstructures and key properties of cold-sprayed and thermally sprayed copper coatings", *Surf. Coatings Technol.* 200 (2006) 4947–4960.

- [18] Z. A. Munir, Surface Oxides and Sintering of Metals, Powder Metallurgy, 24:4, 177-180, 1981 DOI: 10.1179/pom.1981.24.4.177
- [19] Z. A. Munir, "Analytical treatment of the role of surface oxide layers in the sintering of metals", JOURNAL OF MATERIALS SCIENCE 14 (1979) 2733–2740
- [20] I. Kotsakis, P. Fallah, D. Poirier, J. D. Giallonardo, S. Yue, "Influence of particle velocity and size on the quality of cold sprayed copper coatings" (2024), *Under Peer Review*
- [21] Pu Deng, Miao Song, Jingfan Yang, Qingyu Pan, Sarah McAllister, Lin Li, Barton C. Prorok, Xiaoyuan Lou, "On the thermal coarsening and transformation of nanoscale oxide inclusions in 316L stainless steel manufactured by laser powder bed fusion and its influence on impact toughness", Materials Science & Engineering A 835 (2022) 142690
- [22] Lengeler, B., Schilling, W. & Wenzl, H. Deviations from Matthiessen's rule and longitudinal magnetoresistance in cold-worked and neutron-irradiated copper. J Low Temp Phys 2, 237–254 (1970). <https://doi.org/10.1007/BF00628179>
- [23] R Zurcher *et al* 1995 *J. Phys.: Condens. Matter* 7 3515
- [24] Yujuan Li, Yingkang Wei, Xiaotao Luo, Changjiu Li, Ninshu Ma, "Correlating particle impact condition with microstructure and properties of the cold-sprayed metallic deposits", Journal of Materials Science Technology 40 (2020) 185–195
- [25] Yu-Juan Li, Xiao-Tao Luo, Chang-Jiu Li, "Improving deposition efficiency and interparticle bonding of cold sprayed Cu through removing the surficial oxide scale of the feedstock powder",

Surface and Coatings Technology, Volume 407, 15 February 2021, 126709

<https://doi.org/10.1016/j.surfcoat.2020.126709>

[26] R.D. Vengrenovitch, “On the Ostwald ripening theory”, *Acta Metall.* 30 (6) (1982) 1079–1086.

[27] P.W. Voorhees, “The theory of Ostwald ripening”, *J. Stat. Phys.* 38 (1–2) (1985) 231–252.

[28] Mehrer, H., “Diffusion in Solids”. Springer, 2007

[29] A.M. ELWAZRI, R. VARANO, P. WANJARA, S. YUE (2006) EFFECT OF SPECIMEN THICKNESS AND PUNCH DIAMETER IN SHEAR PUNCH TESTING, *Canadian Metallurgical Quarterly*, 45:1, 33-40, DOI: 10.1179/cmqr.2006.45.1.33

[30] R.K. Guduru, K.A. Darling, R. Kishore, R.O. Scattergood, C.C. Koch, K.L. Murty, “Evaluation of mechanical properties using shear–punch testing”, *Materials Science and Engineering A* 395 (2005) 307–314

Acknowledgements

Financial support from the Nuclear Waste Management Organization of Canada (NWMO), the CRITM (Consortium de recherche et d’innovation en transformation metallique), the 5NPlus and the McGill Engineering Doctoral Award (to I. Kotsakis) is gratefully acknowledged. We would like to acknowledge Dr. Lise Guichaoua from the McGill Electron Microscopy Research Group for her support and assistance in the operation of the SU8230 SEM.